10209
NACA TN 3840

TECH LIBRARY KAFB, NM
0066732

NATIONAL ADVISORY COMMITTEE FOR AERONAUTICS

TECHNICAL NOTE 3840

ANALYSIS OF PARTICLE MOTIONS FOR A CLASS OF THREE-DIMENSIONAL INCOMPRESSIBLE LAMINAR BOUNDARY LAYERS

By Arthur G. Hansen and Howard Z. Herzig

Lewis Flight Propulsion Laboratory
Cleveland, Ohio

Washington
November 1956

AFMDC
TECHNICAL LIBRARY
AFL 2811

TECH LIBRARY KAFB, NM
0066732

NATIONAL ADVISORY COMMITTEE FOR AERONAUTICS

TECHNICAL NOTE 3840

ANALYSIS OF PARTICLE MOTIONS FOR A CLASS OF THREE-DIMENSIONAL INCOMPRESSIBLE LAMINAR BOUNDARY LAYERS

By Arthur G. Hansen and Howard Z. Herzig

4199

CC-1

SUMMARY

An analysis is presented for the positions of particles at various time intervals in a three-dimensional incompressible laminar boundary layer on a flat surface for main flows consisting of streamline translates having constant axial velocity. Boundary-layer particles initially arrayed on a line normal to the surface trace out twisted surfaces as they progress downstream. Tables are presented for computing the curves formed by the instantaneous positions of the particles at various time intervals for main-flow streamlines that can be approximated by third-order polynomials.

For viscous-flow problems where it is important to know the length of time a particle remains near a bounding surface, the tables facilitate rapid computation of the residence times of boundary-layer particles for a given flow configuration.

INTRODUCTION

Results obtained in the experimental investigations of secondary flows in turbomachines (refs. 1 to 3) indicate that information concerning three-dimensional laminar boundary-layer behavior can be of practical value in interpreting and correlating measurements of losses in the turbomachines for design purposes. Reference 4 gives a theoretical analysis of the overturning (more than mainstream turning) of the three-dimensional laminar boundary layer developed on flat or nearly flat surfaces, under mainstream flows which consist of streamline translates (i.e., the entire streamline pattern can be obtained by translating any particular streamline parallel to the leading edge, fig. 1) with constant axial velocity component. For such two-dimensional mainstream flows, defined by

$$U = U_0 \quad \text{(a constant)} \tag{1a}$$

$$W = \sum_{i=0}^{m} a_i x^i \tag{1b}$$

The orientation of the coordinate axes is depicted in figure 2. The boundary-layer velocity components found in reference 4 are

$$u = U_0 F'(\eta) \tag{2a}$$

where F satisfies the well-known Blasius equation

$$FF'' + 2F''' = 0 \tag{2b}$$

$$w = \sum_{i=0}^{m} a_i x^i P_i(\eta) \tag{3a}$$

where P_i satisfies the ordinary differential equation

$$P_i'' + \frac{FP_i'}{2} - iF'P_i + i = 0 \tag{3b}$$

with the boundary conditions

$$P_i(0) = 0 \tag{4a}$$

$$\lim_{\eta \to \infty} P_i(\eta) = 1 \tag{4b}$$

Numerical solutions of equations (3) were obtained and tabulated in reference 4 for values of i from 1 to 10. Thus solutions for the boundary-layer flow can be obtained for any main streamline shape that can be reasonably approximated by polynomials up to the eleventh order.

The x-, z-coordinates of a given boundary-layer streamline, identified by a corresponding constant K, may be represented by

$$x = \frac{K}{[F(\eta)]^2} \tag{5a}$$

and

$$z = \sum_{i=0}^{m} \int_{x_0}^{x} a_i^* x^i J_i(\eta) dx + z_0 \tag{5b}$$

4199

where

$$J_i = \frac{P_i}{F'} \tag{6a}$$

(J_i is likewise tabulated in ref. 4) and

$$a_i^* = \frac{a_i}{U_0} \tag{6b}$$

The results of this theoretical analysis were employed in reference 4 to predict the cross-channel boundary-layer flow in a two-dimensional channel for both thick- and thin-boundary-layer flows. These boundary-layer overturnings were then checked experimentally. The close agreement that was obtained between the theoretical and the experimental boundary-layer overturnings indicates that the theoretical assumptions may be considered reasonable for the cases considered by this laminar cross-channel flow theory. Accordingly, this class of flows, for which the mainstream can be represented by approximating polynomials, is used here in investigating the influence of main streamline configurations on boundary-layer behavior.

The present investigation is an extension of reference 4 and develops an analysis that permits a more detailed understanding of the boundary-layer behavior as the boundary layer passes through a flow configuration. In particular, the analysis makes it possible to determine the position of a boundary-layer particle at any given time after it leaves the leading edge. Thus, for example, the subsequent history of particles arrayed in a line normal to the surface at the leading edge can be determined, and the curves (skewed profiles) formed by the instantaneous positions of the particles can be traced out. Tables are provided for rapid calculations of these properties of the boundary-layer flow under main streamline shapes that can be approximated by third-order polynomials.

For viscous-flow problems, in general, where it is important to know the length of time the particles remain near the surface, the tables make possible rapid calculation of the through-flow times of particles for a given configuration.

SYMBOLS

a_i constants, coefficients of polynomials in powers of x

$F, F(\eta)$ Blasius function

1199

CC-4 back

$I(\eta)$	$\int_{\eta}^{\infty} \frac{d\eta}{F^3}$ (eq. (22))
i	constant, $i = 0,1,2, \ldots m$
$J_i, J_i(\eta)$	function of η, $J_i(\eta) = \frac{P_i(\eta)}{F'(\eta)}$
K	constant of integration for stream equation in x,y-plane
k	constant
m	constant
$P_i, P_i(\eta)$	function of η, $w = \sum_{i=0}^{m} a_i x^i P_i(\eta)$
t	time
U,W	mainstream velocity components in x- and z-directions, respectively
U_0	mainstream axial-velocity component
u,v,w	boundary-layer velocity components in the x-, y-, and z-directions, respectively
x,y,z	rectangular coordinates
x_0	constant
Δx	initial axial location of boundary-layer particle near the leading edge
z_0	constant
η	similarity variable, $\eta = y\sqrt{\frac{U_0}{\nu x}}$
η_K	value of η defining final position of particle in boundary layer
ν	coefficient of kinematic viscosity

4199

Subscripts:

K final position of boundary-layer particle

x_1 exit value

Δx initial position near leading edge

1 exit

Superscripts:

$*$ denotes division by U_0

Primes denote differentiation with respect to η

BOUNDARY-LAYER SKEWED-PROFILE ANALYSIS

For a main flow whose streamline translates are described by

$$z = \text{constant} + a_0^* x + \frac{a_1^* x^2}{2} + \ldots + \frac{a_m^* x^{m+1}}{m + 1} \tag{7}$$

boundary-layer streamlines can be determined from equations (5) corresponding to various initial positions in the boundary layer. As an example, several boundary-layer streamlines are plotted in figure 3 (fig. 5, ref. 4) for a mainstream flow represented by

$$z = \text{constant} + \frac{x^2}{2} + \frac{x^4}{8} + \frac{x^6}{16}$$

Figure 3 shows the familiar progressive increase in overturning through the boundary layer. There is no indication in figure 3, however, (or in ref. 4) how far mainstream and boundary-layer particles that start simultaneously from the leading edge travel along their respective paths in a given interval of time t. The present investigation extends the analysis to compare the relative positions of such particles after such an interval of time. For a numerical example the results of the analysis are applied to the main-flow case $z = x^2 + k$. The curve that is then drawn by connecting the final positions of the particles represents a

profile of the travel of the boundary-layer particles. The residence time, the time required for a boundary-layer particle to pass through a particular configuration, can likewise be computed.

Derivation of Equations

Parametric representation of a boundary-layer streamline. - For a given boundary-layer streamline the relation

$$x = \frac{K}{[F(\eta)]^2} \tag{5a}$$

determines $x = x(\eta)$ for all points on the streamline. Differentiating equation (5a) results in

$$dx = \frac{-2K}{F^3} F' d\eta \tag{8}$$

Substitution of equations (5a), (6), and (8) into equation (5b) yields

$$z = -2 \sum_{i=0}^{m} a_i^* K^{i+1} \int_{\eta_0}^{\eta} \frac{P_i}{F^{2i+3}} d\eta + z_0 \tag{9}$$

where η_0 and η correspond to x_0 and x, respectively, along the streamline.

The definition of the Blasius similarity parameter

$$\eta = y\sqrt{\frac{U_0}{\nu x}} \tag{10}$$

and substitution of equation (5a) give

$$y = \sqrt{\frac{\nu}{U_0}} \frac{\eta\sqrt{K}}{F} \tag{11}$$

From equations (5a), (9), and (11) a given boundary-layer streamline is thus given in the parametric form as

$$\left.\begin{aligned} x &= x(\eta,K) \\ z &= z(\eta,K) \\ y &= y(\eta,K) \end{aligned}\right\} \tag{12}$$

Boundary-layer particles at time t. - Because the projection of a boundary-layer streamline in the x,y-plane is determined from the well-known Blasius two-dimensional boundary-layer development (ref. 4), attention here is directed to the projection of the streamline in the x,z-plane. In particular, for a particle in the boundary layer that, starting from the leading edge, has reached an axial position x, equation (5a) determines η corresponding to the axial position x and because η_0 approaches infinity at the leading edge, equation (9) becomes

$$z = -2 \sum_{i=0}^{m} a_i^* K^{i+1} \int_{\infty}^{\eta} \frac{P_i}{F^{2i+3}} d\eta + z_0 \tag{13}$$

For $\eta \geq 8$, good approximations to $F(\eta)$ and $P_i(\eta)$ are, respectively,

$$F(\eta) = \eta - 1.72077 \tag{14a}$$

$$P_i(\eta) = 1.00000 \tag{14b}$$

Equation (13) can then be written

$$z = \sum_{i=0}^{m} 2a_i^* K^{i+1} \left[\int_{\eta}^{8} \frac{P_i}{F^{2i+3}} d\eta + \int_{8}^{\infty} \frac{1}{(\eta - 1.72077)^{2i+3}} \right] d\eta + z_0 \tag{15}$$

Integration of the last term yields

$$z = \sum_{i=0}^{m} 2a_i^* K^{i+1} \left[\int_{\eta}^{8} \frac{P_i}{F^{2i+3}} d\eta + \frac{1}{(2i + 2)(6.27923)^{2i+2}} \right] + z_0 \tag{16}$$

Consider now several particles all at $z = z_0$ but at varying boundary-layer heights (a range of K). All the particles leave the leading edge simultaneously. In order to compare the relative positions (x,z) of these particles after some time interval t, it will be necessary to determine $\eta = \eta_K$ at time t corresponding to each boundary-layer streamline K, and then to evaluate equations (5a) and (16).

Determination of η_K. - Consider a particle in the main flow which has travelled to a point (x_1,z_1). The mainstream particle has a constant axial velocity component U_0. Therefore, the time taken to travel from the leading edge to (x_1,z_1) is simply

$$t = \frac{x_1}{U_0} \tag{17}$$

Next consider a particle in the boundary layer that has travelled from the leading edge for a time t. Along a boundary-layer streamline

$$\frac{dx}{dt} = u = U_0F'(\eta) \tag{18}$$

Substituting from equation (8) gives

$$\frac{-2K}{U_0F^3}\,d\eta = dt \tag{19}$$

and, therefore,

$$\frac{2K}{U_0}\int_\eta^\infty \frac{d\eta}{F^3} = \int_0^t dt = t \tag{20}$$

Assuming that the particles in the mainstream and in the boundary layer start simultaneously and both travel for a time t, then the value of $\eta = \eta_K$ associated with the particle at the end of that time can be determined (from eqs. (20) and (17)) as the solution to the integral equation

$$2K\int_\eta^\infty \frac{d\eta}{F^3} = x_1 \tag{21}$$

Making use again of the approximation (14a), η_K can be determined from

$$I(\eta) \equiv \int_{\eta}^{8} \frac{d\eta}{F^3} = \frac{x_1}{2K} - \frac{1}{2(6.27923)^2} \tag{22}$$

Boundary-layer velocities at time t. - Once η_K has been obtained for a boundary-layer particle on a particular streamline, the velocity components are readily established as functions of η_K:

$$u = U_0 F'(\eta_K) \tag{23a}$$

From equations (2b), (5a), and (6b)

$$w = U_0 \sum_{i=0}^{m} a_i^* \left[\frac{K}{F^2(\eta_K)}\right]^i P_i(\eta_K) \tag{23b}$$

From reference (4)

$$v = \frac{1}{2}\sqrt{\frac{\nu U_0}{x}}\,(\eta F' - F) \tag{2c}$$

Substitution of equation (5a) into equation (2c) gives

$$v = \frac{1}{2}\sqrt{\frac{\nu U_0}{K}}\left[\eta_K F(\eta_K) F'(\eta_K) - F^2(\eta_K)\right] \tag{23c}$$

Tables

The integral $I(\eta)$ has been computed for a range of η from 8.0 to 0.05, and the values are presented in table I. The computation was done by numerical integration using the trapezoidal rule for intervals of η corresponding to the intervals between the consecutive values of η in the table.

The expression $\displaystyle\int_{\eta}^{8} \frac{P_i}{F^{2i+3}}\,d\eta + \frac{1}{(2i+2)(6.27923)^{2i+2}}$ required for use in equation (16) has been evaluated for $i = 1,2,3$ for a range of η from 8.0 to 0.05. The results are presented in table II. It may be

observed that for values of $i > 3$ at small η the quantity $\frac{P_i}{F^{2i+3}}$ becomes very large $\left(\eta = 0.05, \frac{P_3}{F^9} \approx 3.8\times10^{29}\right)$ while the quantity K^{i+1} (eq. (16)) becomes very small $\left(\text{from eq. (22), for } i = 3 \text{ when } \eta_K = 0.05, K^4 \approx \frac{x_1^4}{2.4\times10^{35}}\right)$. These factors combine to restrict the practical range of i (and hence the order of the approximating polynomial (eq. (5b)) that may be used. More accurate values of $F(\eta)$ than are generally available were required for these computations. Accordingly, these values are likewise presented in table I.

4194

Numerical Example

The method described has been applied to the case of mainstream flow defined by

$$z = x^2 + k$$

from the leading edge to $x_1 = 1/2$, corresponding to 45° turning (fig. 4). The computing procedure is outlined briefly in the following paragraphs:

Evaluate the right side of equation (22) for $x_1 = 1/2$,

$$I(\eta_K) = \frac{1}{4K} - \frac{1}{2(6.27923)^2} \tag{24}$$

for a range of values of K. In this numerical example values of K = 19, 10, 1, 0.5, 0.4, 0.3, 0.2, 0.1, 0.09, 0.07, 0.05, 0.02, 0.005, 0.0005, 0.0003, and 0.0002 were chosen. For each value of $I(\eta_K)$, find the value of $\eta = \eta_K$ in table I.

For this example, equation (7) requires that

$$\left.\begin{aligned} m &= 1 \\ a_0^* &= 0 \\ a_1^* &= 2 \end{aligned}\right\} \tag{25}$$

The x-, z-coordinates for the particles in the boundary layers when the mainstream particle is at x_1 may now be obtained from equations (5a) and (16) which, for this example, become

$$x_K = \frac{K}{F^2(\eta_K)} \tag{26}$$

$$z_K = 4K^2 \left[\int_{\eta_K}^{8} \frac{P_1}{F^5} \, d\eta + \frac{1}{4(6.27923)^4} \right] \tag{27}$$

The coordinates of the boundary-layer particles at the time $t = \frac{x_1}{U_0}$ when the mainstream particle reaches the axial position $x_1 = 0.5$ have been computed from equations (26), (27), and table II; and the results are plotted in figure 5, as a boundary-layer profile curve projected on the surface. Figure 6 illustrates that the skewed profile is actually a three-dimensional curve in space.

DISCUSSION

Skewed Boundary-Layer Profile

It may be observed in figures 5 and 6 how fluid particles that were all arrayed in a line normal to the surface at the inlet have fanned out to form a twisted curve (skewed profile) after a time interval t. A mainstream flow path and the limiting boundary-layer position (line of maximum flow deflection directly on the surface) are likewise shown in figures 5 and 6 for comparison. It is interesting to note that the boundary-layer particles on the streamlines designated by $K = 1$, 0.5, 0.4, and 0.3 have actually travelled farther in the z-direction than have mainstream particles in the same period of time. This indicates that the tangential component of velocity in the boundary layer can and does surpass the tangential velocity in the mainstream overhead. This phenomenon is likewise noted in reference 4.

The velocity components of a particle in the boundary layer at time t may be determined by equations (23).

4199

CC-2, back

Residence Time of Particles in Boundary Layer

For such mainstream flows as are being considered here with flow uniformity in the z-direction and constant axial velocity U_0, the time required for a boundary-layer particle to pass through a given configuration (residence time) depends only upon the axial velocity U_0, the axial length of the configuration, and the η position of the particle in the boundary layer. The residence time may be calculated readily by the use of $I(\eta)$, evaluated in table I.

From equations (20) and (14) the residence time of a boundary-layer particle is expressed as a function of η at x_1, the exit of the configuration,

$$t = \frac{2K}{U_0}\left[\int_{\eta_{x_1}}^{8} \frac{d\eta}{F^3} + \frac{1}{2(6.27923)^2}\right] \tag{28}$$

This may be expressed for convenience as the ratio of the residence time of a boundary-layer particle to the residence time of the main flow using equation (17):

$$\frac{t_{\text{boundary layer}}}{t_{\text{mainstream}}} = \frac{2K}{x_1}\left[\int_{\eta_{x_1}}^{8} \frac{d\eta}{F^3} + \frac{1}{2(6.27923)^2}\right] \tag{29}$$

Equations (28) and (29) find the residence time in terms of the η position at the exit x_1. It may be convenient to determine the residence times of particles in terms of their positions in the boundary layer at the inlet. However, η is not properly defined at the leading edge. Nevertheless, the residence time can be calculated for a particle at any given η in the boundary layer at some axial position Δx close to the leading edge. From equation (5a) for a given streamline

$$F_{x_1} = F_{\Delta x}\sqrt{\frac{\Delta x}{x_1}} \tag{30}$$

The residence time for a boundary-layer particle at a given η near the leading edge may then be computed by first using equations (5a) and (30) and the F tables (ref. 4) to find η_{x_1} and then using table I for values of $I(\eta)$ to evaluate equations (28) or (29). In the present numerical example, for the boundary-layer streamlines corresponding to $\eta = 6.4$, 4.8, 3.2, and 1.6 at $\Delta x = 0.01$ (fig. 3), the ratios of the boundary layer to mainstream through-flow times are 1.069, 1.577, 2.148, and 4.105, respectively.

CONCLUDING REMARKS

An analysis is presented that describes the positions of individual particles at various time intervals in the three-dimensional incompressible laminar boundary layer developed on a flat (or slightly curved) surface under a main flow of streamline translates with constant axial velocity. Boundary-layer particles arrayed normal to the surface near the inlet are found to fan out forming a skewed curve. Tables are presented which facilitate rapid calculation of detailed boundary-layer information for main streamlines that can be described by third-order polynomials. A numerical example for main flow

4199

$$z = x^2 + k$$

is computed for demonstration purposes. The profile curve of this example illustrates a case in which tangential velocity components in the boundary layer exceed those of the local mainstream (similarly noted in ref. 4).

For viscous-flow problems where it is important to know the duration of time a particle remains near the surface, use of the tables makes it possible to determine quickly the residence time of the chosen particle for a given flow configuration. The residence time can be computed either in terms of the final boundary-layer height of a particle at the exit of the flow configuration or in terms of its initial position. For the main-flow case $z = x^2 + k$ with a turning of 45°, the residence times of particles at positions corresponding initially to $\eta = 6.4$, 4.8, 3.2, and 1.6 (nearly mainstream, 3/4, 1/2, and 1/4 boundary-layer height) respectively) were 1.069, 1.577, 2.148, and 4.105 times the mainstream residence time, respectively.

Lewis Flight Propulsion Laboratory
National Advisory Committee for Aeronautics
Cleveland, Ohio, August 14, 1956

REFERENCES

1. Herzig, Howard Z., Hansen, Arthur G., and Costello, George R.: A Visualization Study of Secondary Flows in Cascades. NACA Rep. 1163, 1954. (Supersedes NACA TN 2947.)

2. Rohlik, Harold E., Kofskey, Milton G., Allen, Hubert W., and Herzig, Howard Z.: Secondary Flows and Boundary-Layer Accumulations in Turbine Nozzles. NACA Rep. 1168, 1954. (Supersedes NACA TN's 2871, 2909, and 2989.)

3. Kofskey, Milton G., and Allen, Hubert W.: Smoke Study of Nozzle Secondary Flows in a Low-Speed Turbine. NACA TN 3260, 1954.

4. Hansen, Arthur G., and Herzig, Howard Z.: Cross Flows in Laminar Incompressible Boundary Layers. NACA TN 3651, 1956.

TABLE I. - $I_\eta = \int_\eta^8 \frac{d\eta}{F^3}$

η	F	$I(\eta)$	η	F	$I(\eta)$	η	F	$I(\eta)$
8.0	6.27923	0	4.3	2.59499	0.062212	1.80	5.29521×10^{-1}	2.58098
7.9	6.17923	.00041387	4.2	2.49805	.068281	1.75	5.01138×10^{-1}	2.94800
7.8	6.07924	.00084834	4.1	2.40162	.075098	1.70	4.73472×10^{-1}	3.38217
7.7	5.97924	.0013048	4.0	2.30576	.082786	1.65	4.46530×10^{-1}	3.89851
7.6	5.87924	.0017847	3.9	2.21053	.091494	1.60	4.20323×10^{-1}	4.51596
7.5	5.77924	.0022898	3.8	2.11604	.10140	1.55	3.94857×10^{-1}	5.25871
7.4	5.67924	.0028218	3.7	2.02234	.11272	1.50	3.70140×10^{-1}	6.15778
7.3	5.57924	.0033827	3.6	1.92953	.12575	1.45	3.46180×10^{-1}	7.25337
7.2	5.47925	.0039745	3.5	1.83771	.14074	1.40	3.22983×10^{-1}	8.59798
7.1	5.37925	.0045997	3.4	1.74698	.15818	1.35	3.00556×10^{-1}	1.02608×10
7.0	5.27926	.0052607	3.3	1.65739	.17854	1.30	2.78904×10^{-1}	1.23339×10
6.9	5.17927	.0059604	3.2	1.56910	.20246	1.25	2.58034×10^{-1}	1.49416×10
6.8	5.07928	.0067019	3.1	1.48221	.23076	1.20	2.37950×10^{-1}	1.82524×10
6.7	4.97929	.0074885	3.0	1.39682	.26446	1.15	2.18658×10^{-1}	2.24992×10
6.6	4.87931	.0083239	2.95	1.35472	.28369	1.10	2.00161×10^{-1}	2.80080×10
6.5	4.77933	.0092123	2.90	1.31304	.30479	1.05	1.82465×10^{-1}	3.52415×10
6.4	4.67937	.010158	2.85	1.27179	.32799	1.00	1.65573×10^{-1}	4.48652×10
6.3	4.57942	.011167	2.80	1.23098	.35354	.95	1.49488×10^{-1}	5.78558×10
6.2	4.47947	.012244	2.75	1.19064	.38176	.90	1.34214×10^{-1}	7.56820×10
6.1	4.37955	.013395	2.70	1.15077	.41297	.85	1.19753×10^{-1}	1.00586×10^{2}
6.0	4.27964	.014628	2.65	1.11139	.44759	.80	1.06109×10^{-1}	1.36066×10^{2}
5.9	4.17975	.015951	2.60	1.07251	.48606	.75	9.32828×10^{-2}	1.87790×10^{2}
5.8	4.07990	.017372	2.55	1.03415	.52893	.70	8.12774×10^{-2}	2.65149×10^{2}
5.7	3.98007	.018901	2.50	9.96316×10^{-1}	.57682	.65	7.00942×10^{-2}	3.84315×10^{2}
5.6	3.88031	.020550	2.45	9.59027×10^{-1}	.63044	.60	5.97350×10^{-2}	5.74242×10^{2}
5.5	3.78059	.022331	2.40	9.22295×10^{-1}	.69064	.55	5.02008×10^{-2}	8.89168×10^{2}
5.4	3.68093	.024259	2.35	8.86133×10^{-1}	.75844	.50	4.14930×10^{-2}	1.43684×10^{3}
5.3	3.58136	.026350	2.30	8.50554×10^{-1}	.83509	.45	3.36125×10^{-2}	2.44530×10^{3}
5.2	3.48188	.028623	2.25	8.15571×10^{-1}	.92171	.40	2.65600×10^{-2}	4.43775×10^{3}
5.1	3.38252	.031100	2.20	7.81197×10^{-1}	1.02024	.35	2.03362×10^{-2}	8.74268×10^{3}
5.0	3.28329	.033804	2.15	7.47444×10^{-1}	1.13255	.30	1.49415×10^{-2}	1.92098×10^{4}
4.9	3.18422	.036766	2.10	7.14324×10^{-1}	1.26101	.25	1.03764×10^{-2}	4.90674×10^{4}
4.8	3.08533	.040017	2.05	6.81848×10^{-1}	1.40846	.20	6.64104×10^{-3}	1.56811×10^{5}
4.7	2.98667	.043596	2.00	6.50028×10^{-1}	1.57834	.15	3.73563×10^{-3}	7.20522×10^{5}
4.6	2.88826	.047548	1.95	6.18874×10^{-1}	1.77484	.10	1.66029×10^{-3}	6.66403×10^{6}
4.5	2.79015	.051925	1.90	5.88399×10^{-1}	2.00303	.05	4.15074×10^{-4}	3.49557×10^{8}
4.4	2.69237	.056789	1.85	5.58611×10^{-1}	2.26918			

4199

TABLE II. - $\displaystyle\int_{\eta}^{8} \frac{P_i}{F^{2i+3}}\, d\eta + \frac{1}{(2i + 2)(6.27923)^{2i+2}}$

η	i=1	i=2	i=3	η	i=1	i=2	i=3	η	i=1	i=2	i=3
8.0	1.60810×10^{-4}	2.71900×10^{-6}	5.17197×10^{-8}	4.3	5.65931×10^{-3}	5.66577×10^{-4}	6.36237×10^{-5}	1.80	5.84759	1.67871×10^{1}	5.06379×10^{1}
7.9	1.71482×10^{-4}	2.99427×10^{-6}	5.88212×10^{-8}	4.2	6.62323×10^{-3}	7.16871×10^{-4}	8.69636×10^{-5}	1.75	7.45971	2.39738×10^{1}	8.15151×10^{1}
7.8	1.83054×10^{-4}	3.30257×10^{-6}	6.70368×10^{-8}	4.1	7.79815×10^{-3}	9.15148×10^{-4}	1.20258×10^{-4}	1.70	9.58409	3.49508×10^{1}	1.33086×10^{2}
7.7	1.95618×10^{-4}	3.64853×10^{-6}	7.65644×10^{-8}	4.0	9.24051×10^{-3}	1.17937×10^{-3}	1.68364×10^{-4}	1.65	1.24058×10^{1}	5.14453×10^{1}	2.20537×10^{2}
7.6	2.09279×10^{-4}	4.03748×10^{-6}	8.76408×10^{-8}	3.9	1.10245×10^{-2}	1.53524×10^{-3}	2.38823×10^{-4}	1.60	1.61851×10^{1}	7.65341×10^{1}	3.71231×10^{2}
7.5	2.24153×10^{-4}	4.47564×10^{-6}	1.00551×10^{-7}	3.8	1.32485×10^{-2}	2.01994×10^{-3}	3.43511×10^{-4}	1.55	2.12919×10^{1}	1.15190×10^{2}	6.35343×10^{2}
7.4	2.40372×10^{-4}	4.97026×10^{-6}	1.15638×10^{-7}	3.7	1.60442×10^{-2}	2.68795×10^{-3}	5.01424×10^{-4}	1.50	2.82578×10^{1}	1.75571×10^{2}	1.10664×10^{3}
7.3	2.58085×10^{-4}	5.52980×10^{-6}	1.33319×10^{-7}	3.6	1.95892×10^{-2}	3.62014×10^{-3}	7.43457×10^{-4}	1.45	3.78549×10^{1}	2.71266×10^{2}	1.98390×10^{3}
7.2	2.77459×10^{-4}	6.16420×10^{-6}	1.54097×10^{-7}	3.5	2.41256×10^{-2}	4.93817×10^{-3}	1.12073×10^{-3}	1.40	5.12182×10^{1}	4.25294×10^{2}	3.55528×10^{3}
7.1	2.98685×10^{-4}	6.88521×10^{-6}	1.78591×10^{-7}	3.4	2.99870×10^{-2}	6.82769×10^{-3}	1.71936×10^{-3}	1.35	7.00389×10^{1}	6.77354×10^{2}	6.57450×10^{3}
7.0	3.21980×10^{-4}	7.70649×10^{-6}	2.07548×10^{-7}	3.3	3.76371×10^{-2}	9.57621×10^{-3}	2.68723×10^{-3}	1.30	9.68706×10^{1}	1.09722×10^{3}	1.24379×10^{4}
6.9	3.47592×10^{-4}	8.64422×10^{-6}	2.41890×10^{-7}	3.2	4.77282×10^{-2}	1.36360×10^{-2}	4.28341×10^{-3}	1.25	1.35628×10^{2}	1.81005×10^{3}	2.41141×10^{4}
6.8	3.75801×10^{-4}	9.71778×10^{-6}	2.82755×10^{-7}	3.1	6.11880×10^{-2}	1.97306×10^{-2}	6.97149×10^{-3}	1.20	1.92409×10^{2}	3.04544×10^{3}	4.80031×10^{4}
6.7	4.06931×10^{-4}	1.09501×10^{-5}	3.31551×10^{-7}	3.0	7.93528×10^{-2}	2.90365×10^{-2}	1.15998×10^{-2}	1.15	2.76878×10^{2}	5.23460×10^{3}	9.83315×10^{4}
6.6	4.41352×10^{-4}	1.23687×10^{-5}	3.90027×10^{-7}	2.95	9.06982×10^{-2}	3.53753×10^{-2}	1.50195×10^{-2}	1.10	4.04642×10^{2}	9.20880×10^{3}	2.07788×10^{5}
6.5	4.79491×10^{-4}	1.40064×10^{-5}	4.60364×10^{-7}	2.90	1.03997×10^{-1}	4.33091×10^{-2}	1.95812×10^{-2}	1.05	6.01426×10^{2}	1.66163×10^{4}	4.54243×10^{5}
6.4	5.21842×10^{-4}	1.59028×10^{-5}	5.45296×10^{-7}	2.85	1.19635×10^{-1}	5.32869×10^{-2}	2.57038×10^{-2}	1.00	9.10598×10^{2}	3.08278×10^{4}	1.03067×10^{6}
6.3	5.68975×10^{-4}	1.81053×10^{-5}	6.48267×10^{-7}	2.80	1.38087×10^{-1}	6.58965×10^{-2}	3.39738×10^{-2}	.95	1.40707×10^{3}	5.89737×10^{4}	2.43652×10^{6}
6.2	6.21552×10^{-4}	2.06723×10^{-5}	7.73635×10^{-7}	2.75	1.59934×10^{-1}	8.19129×10^{-2}	4.52182×10^{-2}	.90	2.22384×10^{3}	1.18713×10^{5}	6.02783×10^{6}
6.1	6.80348×10^{-4}	2.36741×10^{-5}	9.26946×10^{-7}	2.70	1.85892×10^{-1}	1.02362×10^{-1}	6.06105×10^{-2}	.85	3.60416×10^{3}	2.39894×10^{5}	1.56879×10^{7}
6.0	7.46266×10^{-4}	2.71971×10^{-5}	1.11529×10^{-6}	2.65	2.16848×10^{-1}	1.28610×10^{-1}	8.18281×10^{-2}	.80	6.00821×10^{3}	5.14476×10^{5}	4.32193×10^{7}
5.9	8.20369×10^{-4}	3.13472×10^{-5}	1.34780×10^{-6}	2.60	2.53903×10^{-1}	1.62487×10^{-1}	1.11286×10^{-1}	.75	1.03400×10^{4}	1.15763×10^{6}	1.26979×10^{8}
5.8	9.03907×10^{-4}	3.62553×10^{-5}	1.63627×10^{-6}	2.55	2.98429×10^{-1}	2.06457×10^{-1}	1.52489×10^{-1}	.70	1.84526×10^{4}	2.75141×10^{6}	4.01468×10^{8}
5.7	9.98361×10^{-4}	4.20839×10^{-5}	1.99607×10^{-6}	2.50	3.52146×10^{-1}	2.63861×10^{-1}	2.10562×10^{-1}	.65	3.43346×10^{4}	6.96504×10^{6}	1.38121×10^{9}
5.6	1.10549×10^{-3}	4.90356×10^{-5}	2.44733×10^{-6}	2.45	4.17220×10^{-1}	3.39259×10^{-1}	2.93058×10^{-1}	.60	6.70666×10^{4}	1.89743×10^{7}	5.24305×10^{9}
5.5	1.22738×10^{-3}	5.73646×10^{-5}	3.01660×10^{-6}	2.40	4.96384×10^{-1}	4.38902×10^{-1}	4.11209×10^{-1}	.55	1.38721×10^{5}	5.63622×10^{7}	2.23480×10^{10}
5.4	1.36656×10^{-3}	6.73915×10^{-5}	3.73916×10^{-6}	2.35	5.93113×10^{-1}	5.71437×10^{-1}	5.81856×10^{-1}	.50	3.07268×10^{5}	1.85690×10^{8}	1.09439×10^{11}
5.3	1.52604×10^{-3}	7.95232×10^{-5}	4.66217×10^{-6}	2.30	7.11840×10^{-1}	7.48895×10^{-1}	8.30480×10^{-1}	.45	7.39807×10^{5}	6.94059×10^{8}	6.34501×10^{11}
5.2	1.70948×10^{-3}	9.42793×10^{-5}	5.84926×10^{-6}	2.25	8.58253×10^{-1}	9.88140×10^{-1}	1.19600	.40	1.97618×10^{6}	3.03559×10^{9}	4.53819×10^{12}
5.1	1.92132×10^{-3}	1.12328×10^{-4}	7.38686×10^{-6}	2.20	1.03969	1.31298	1.73824	.35	6.02916×10^{6}	1.62311×10^{10}	4.24290×10^{13}
5.0	2.16701×10^{-3}	1.34533×10^{-4}	9.39347×10^{-6}	2.15	1.26566	1.75733	2.55122	.30	2.19376×10^{7}	1.13196×10^{11}	9.46399×10^{14}
4.9	2.45318×10^{-3}	1.62023×10^{-4}	1.20329×10^{-5}	2.10	1.54858	2.36982	3.78153	.25	1.01921×10^{8}	1.13926×10^{12}	1.35767×10^{16}
4.8	2.78810×10^{-3}	1.96276×10^{-4}	1.55337×10^{-5}	2.05	1.90474	3.22084	5.66347	.20	6.79386×10^{8}	1.96143×10^{13}	5.33082×10^{17}
4.7	3.18201×10^{-3}	2.39253×10^{-4}	2.02181×10^{-5}	2.00	2.35566	4.41315	8.57380	.15	8.11319×10^{9}	7.93459×10^{14}	7.07569×10^{19}
4.6	3.64769×10^{-3}	2.93569×10^{-4}	2.65444×10^{-5}	1.95	2.92992	6.09816	1.31261×10^{1}	.10	2.86133×10^{11}	1.52313×10^{17}	7.07684×10^{22}
4.5	4.20126×10^{-3}	3.62745×10^{-4}	3.51723×10^{-5}	1.90	3.66582	8.50109	2.03323×10^{1}	.05	1.41891×10^{14}	1.26472×10^{21}	9.51275×10^{27}
4.4	4.86513×10^{-3}	4.51561×10^{-4}	4.70613×10^{-5}	1.85	4.61499	1.19605×10^{1}	3.18822×10^{1}				

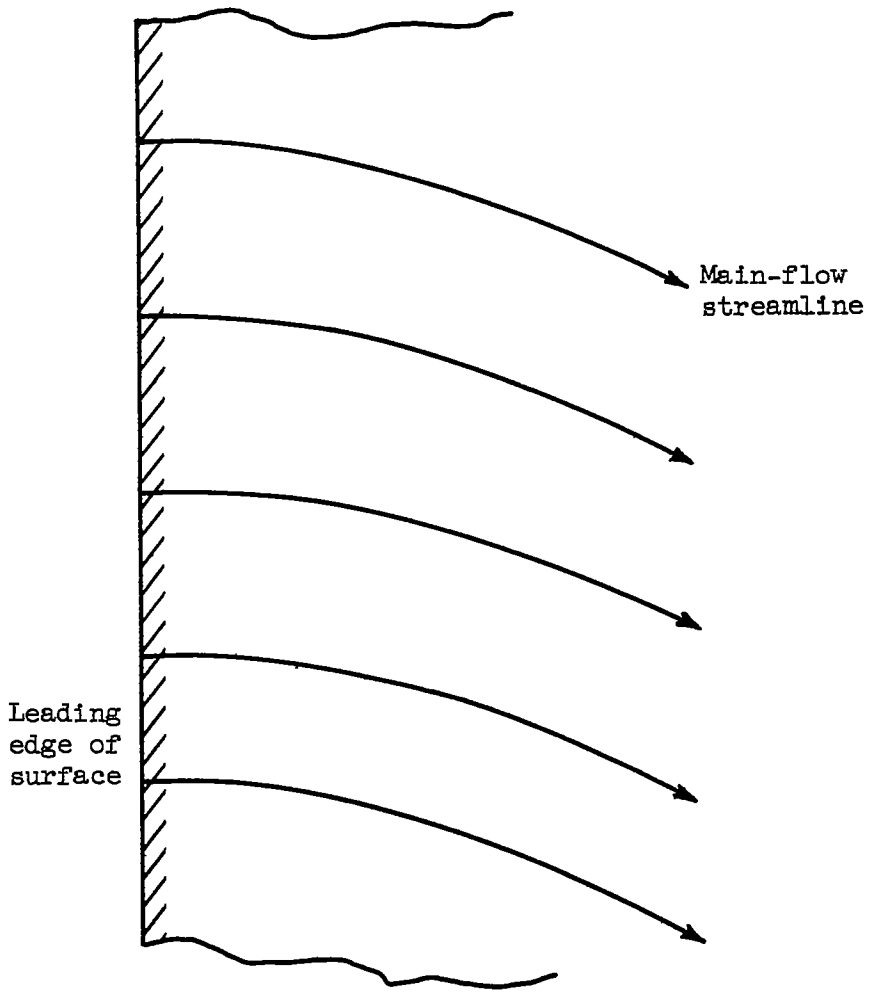

Figure 1. - Streamline pattern as system of translates.

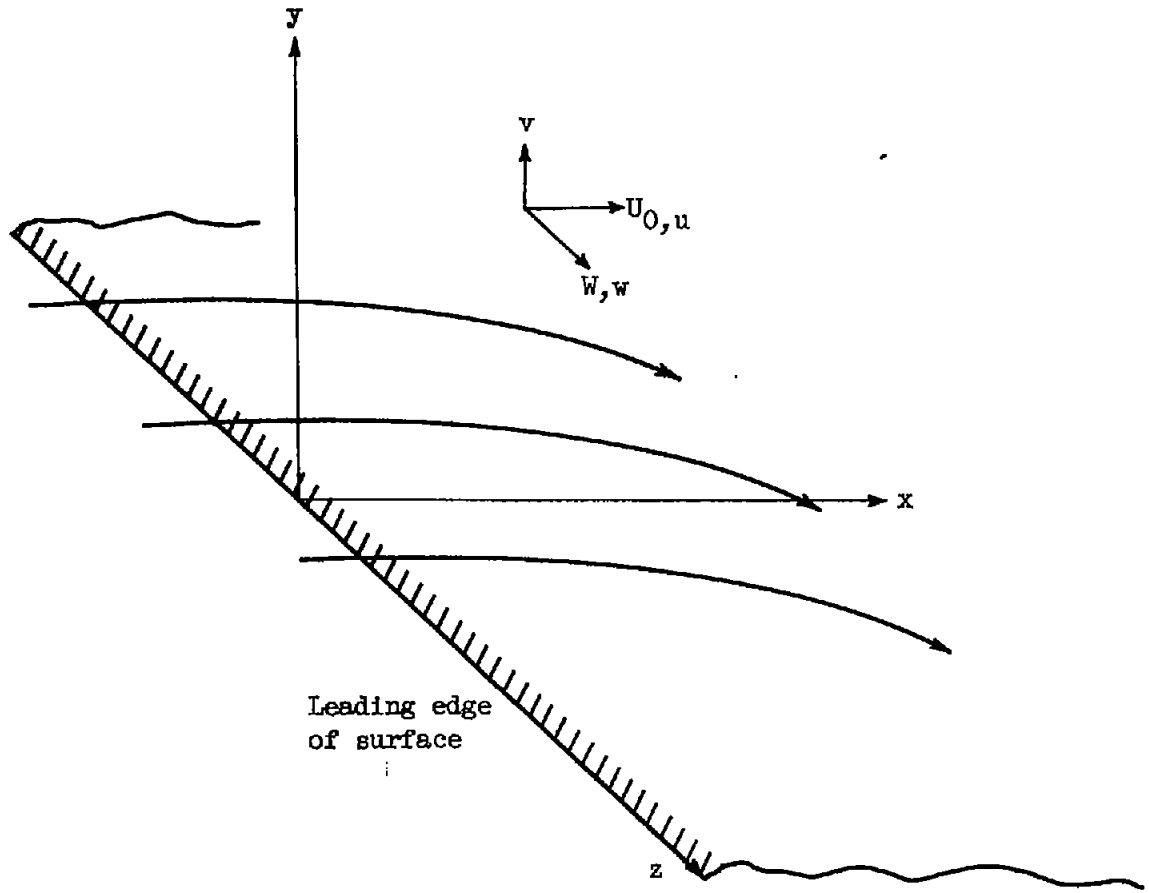

Figure 2. - Coordinate axes for flow over surface.

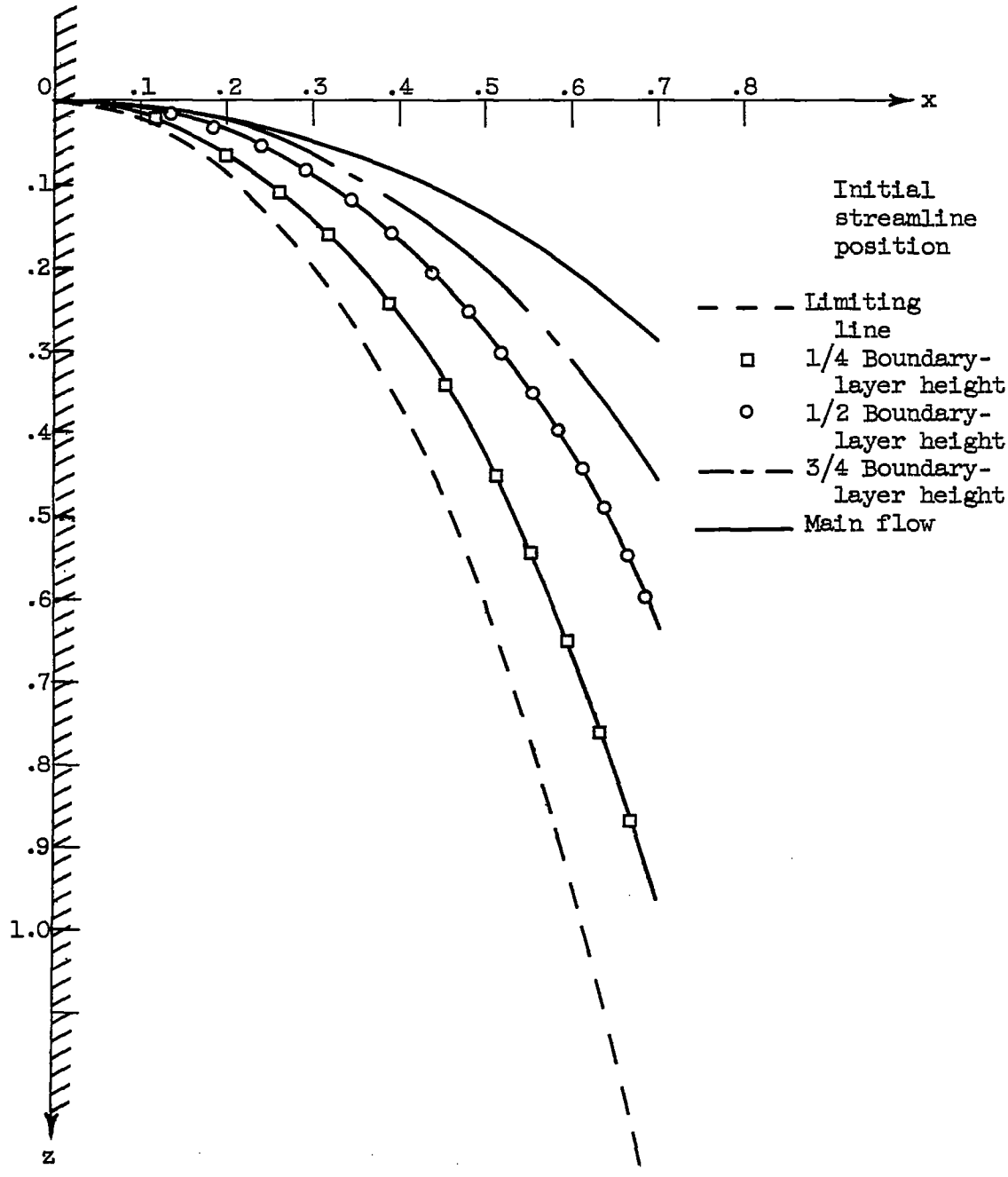

Figure 3. - Boundary-layer streamlines for circular-arc flow (fig. 5, ref. 4).

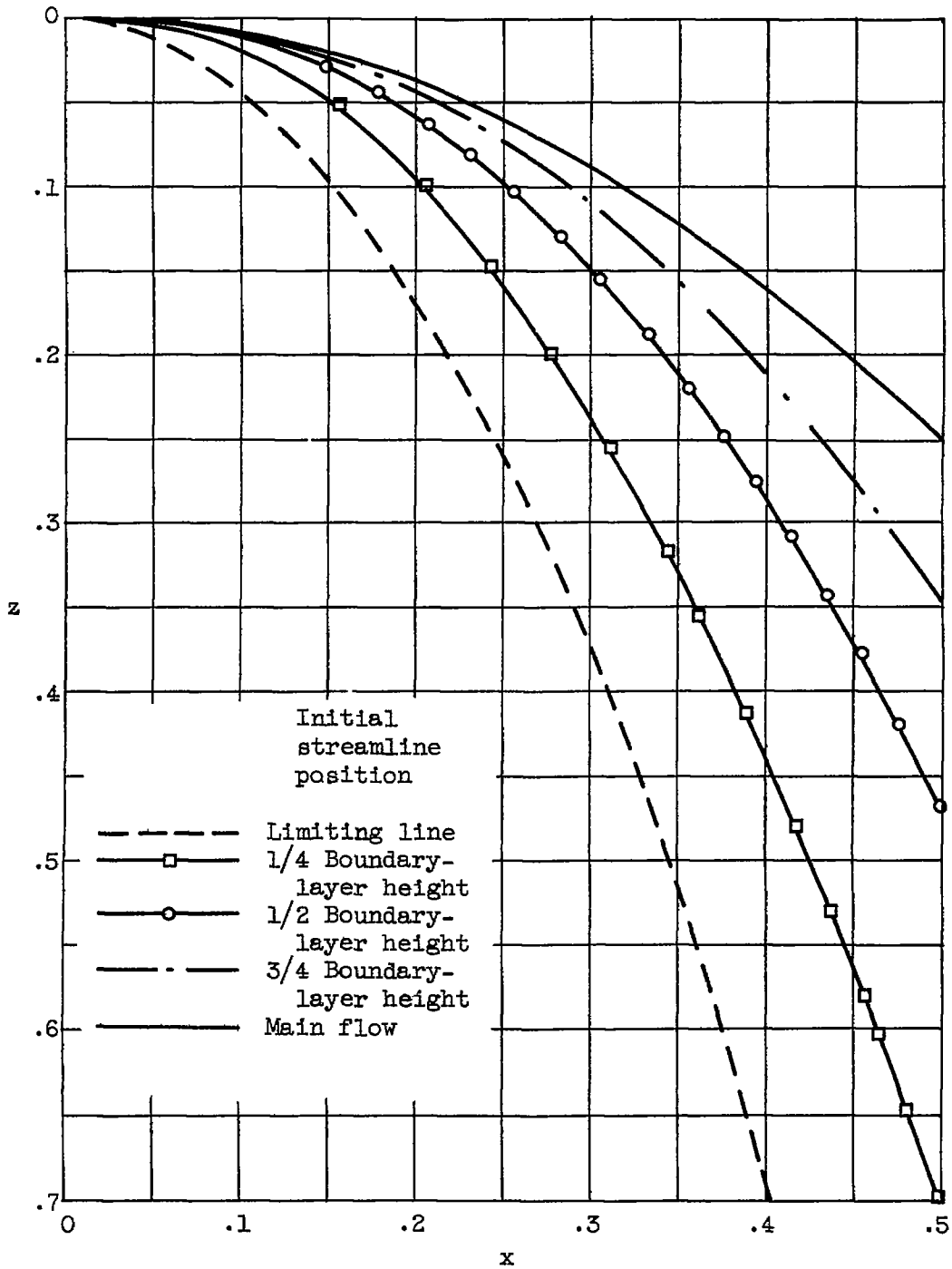

Figure 4. - Boundary-layer streamlines.

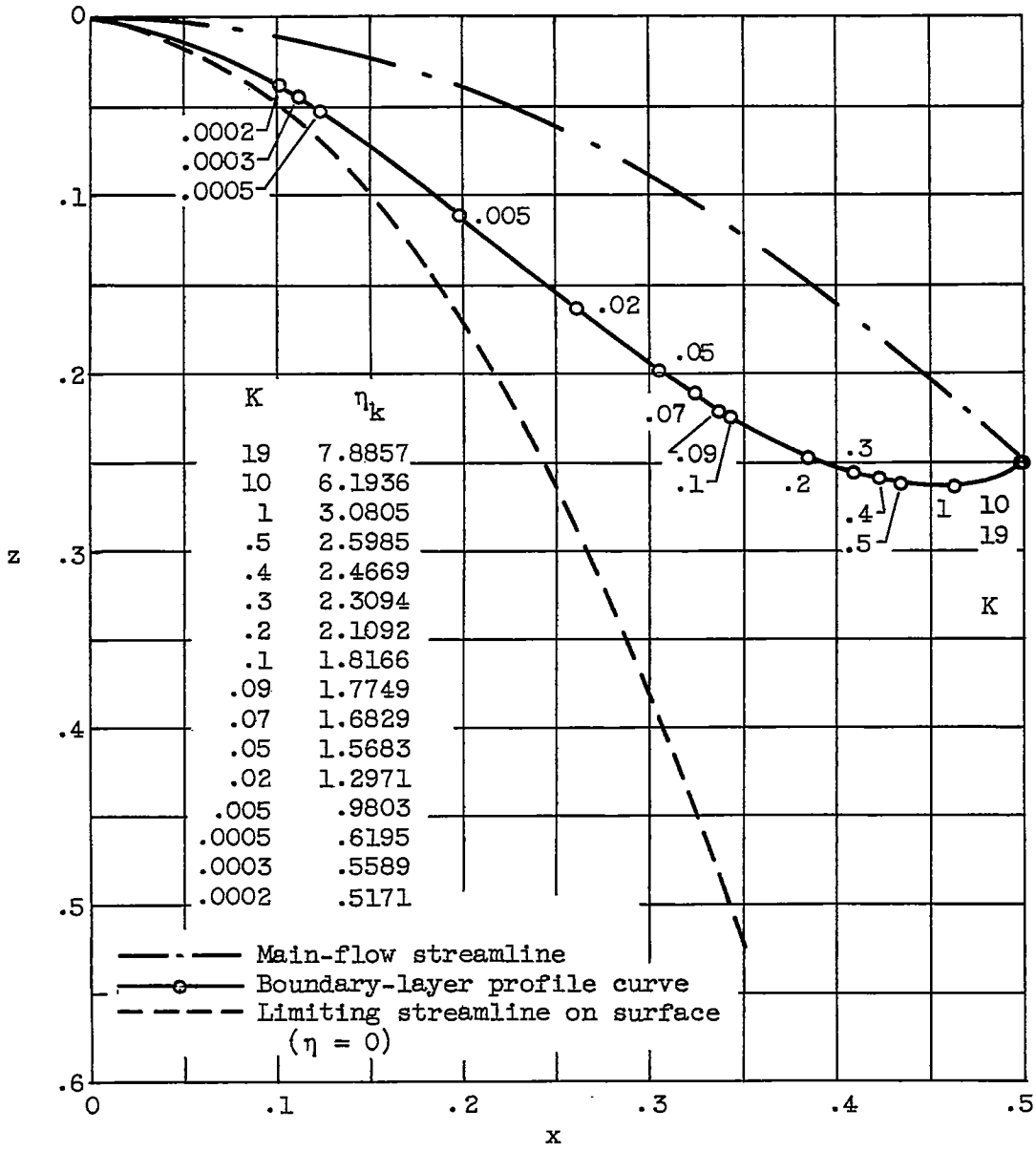

Figure 5. - Boundary-layer profile curve at time $t = 0.5/U_0$.

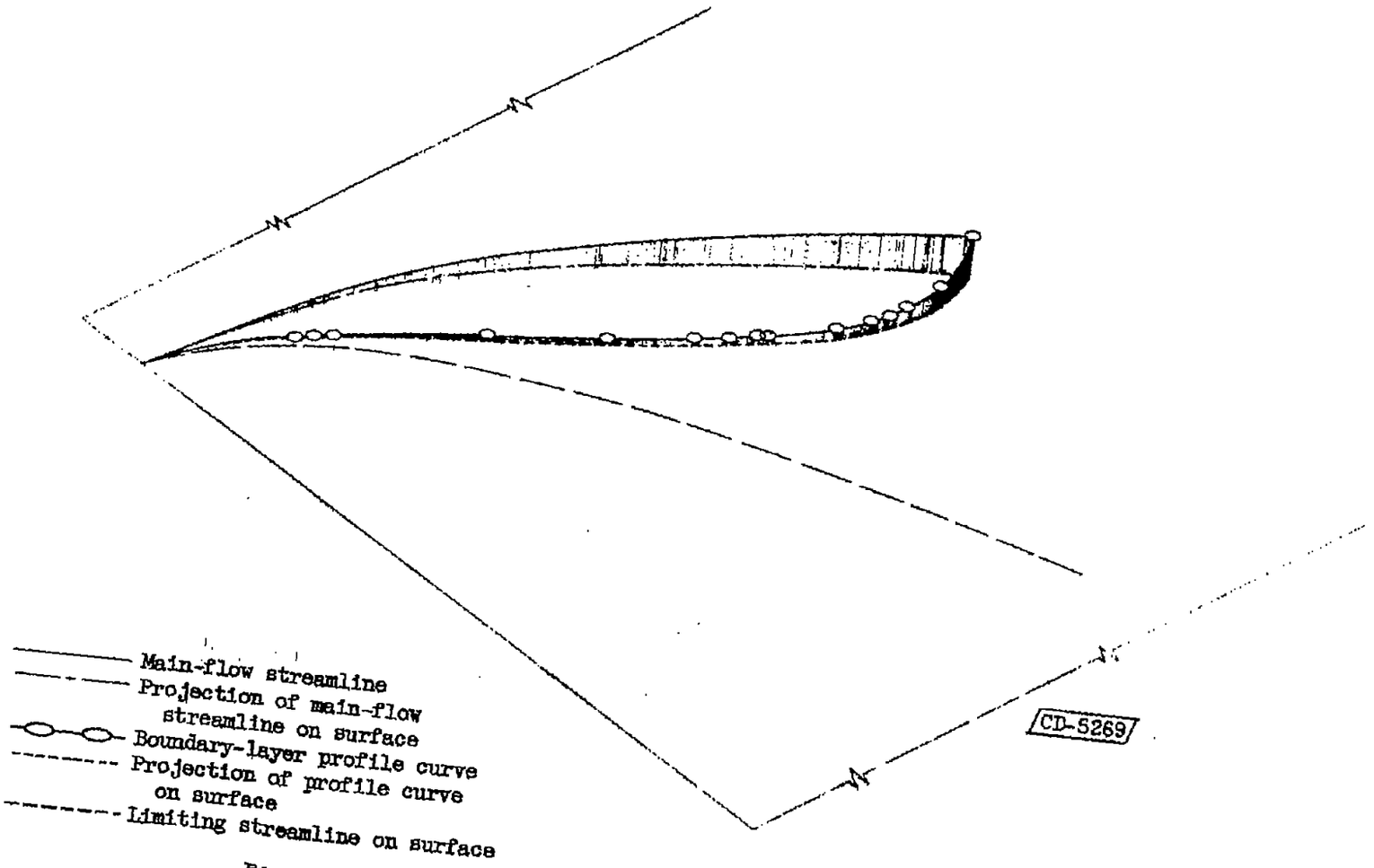

Figure 6. - Three-dimensional sketch of boundary-layer profile curve.